

High-Performance Inverse Artificial Neural Network Controller for Asynchronous Motor Control

Article Info:

Article history: Received 2024-10-10 / Accepted 2024-12-12 / Available online 2024-12-16

doi: 10.18540/jcecv110iss9pp20857



Benyekhlelf Kada

ORCID: <https://orcid.org/0009-0005-4126-1295>

Department of Electrotechnical, University Mustapha Stambouli of Mascara. Mascara, Algeria.

LIS2T Laboratory, University Mustapha Stambouli of Mascara. Algeria

E-mail: k.benyakhelef@univ-mascara.dz

Mourad Hebali

ORCID: <https://orcid.org/0000-0001-6004-4513>

Department of Electrotechnical, University Mustapha Stambouli of Mascara. Mascara, Algeria.

LIS2T Laboratory, University Mustapha Stambouli of Mascara. Algeria

E-mail: mourad.hebali@univ-mascara.dz

Ibrahim Farouk Bouguenna

ORCID: <https://orcid.org/0000-0001-8631-8172>

Department of Electrotechnical, University Mustapha Stambouli of Mascara. Mascara, Algeria.

LIS2T Laboratory, University Mustapha Stambouli of Mascara. Algeria

E-mail: i.bouguenna@univ-mascara.dz

Benaoumeur Ibari

ORCID: <https://orcid.org/0000-0001-6004-4513>

Department of Electrotechnical, University Mustapha Stambouli of Mascara. Mascara, Algeria.

LIS2T Laboratory, University Mustapha Stambouli of Mascara. Algeria

E-mail: b.ibari@univ-mascara.dz

Menouer Bennaoum

ORCID: <https://orcid.org/0009-0000-8643-5125>

Department of Electrotechnical, University Mustapha Stambouli of Mascara. Mascara, Algeria.

LIS2T Laboratory, University Mustapha Stambouli of Mascara. Algeria

E-mail: m.bennaoum@univ-mascara.dz

Abstract

Induction motor (IM) is considered one of the most important machines in industrial applications, which requires precise and effective control of its behavior in order to improve its performance. In this paper, three control strategies based on the development of inverse artificial neural networks (IANNs) were proposed in order to control the current (I_{as}), electromagnetic torque (C_e), and speed (ω_r) of an asynchronous machine IM. These inverse artificial neural networks have been learned from conventional control system (PI controller and vector control) data using MATLAB software. Comparison between the responses of both the classical controller and the IANNs showed the ability and effectiveness of the latter in precisely controlling the three properties of the asynchronous motor, and it also achieved better dynamic motor behavior, speed without overtaking, and good load disturbance rejection, which proves the high performance of these developed IANNs.

Keywords: Induction Motor, PI-Controller, Vector Control, Inverse ANNs

Nomenclature

$[V_s]$	Stator voltage Vector
$[V_r]$	Rotor voltage Vector
$[I_s]$	Stator current Vector
$[I_r]$	Rotor current Vector
$[\phi_s]$	Stator flux Vector
$[\phi_r]$	Rotor flux Vector
I_{ds} and I_{qs}	d and q axis components of the stator current
I_{dr} and I_{qr}	d and q axis component of the rotor current
V_{ds} and V_{qs}	d and q axis components of the stator voltage.
L_m [H]	Stator-Rotor mutual inductance
L_s [H]	Stator's own cyclic inductance
L_r [H]	Rotor's own cyclic inductance
R_s [Ω]	Stator resistance
R_r [Ω]	Rotor resistance
IM	Induction Motor
MAS	Asynchronous Machine
ANN	Artificial Neural Network
FFNNM	Structure of the Feed Forward Neural Network Model
p	Number of pole pairs
[P]	Park Matrix

1. Introduction

In recent years, interest in asynchronous machines (induction motors IM) has increased very significant due to their widespread use in industrial applications (Mekrini & Bri, 2018; Kouadria *et al.*, 2024) and in various sectors such as automotive, railways, mining and even in the gas and oil sectors (Atif *et al.*, 2024; Shekher *et al.*, 2024). In addition, these asynchronous motors have interesting advantages such as durability, reliability, simple construction, relatively low cost, and less maintenance, as well as being available for all power ratings (Kouadria *et al.*, 2024; EL-Merrassi *et al.*, 2022; Chandrasekaran *et al.*, 2021).

Induction motors require precise control of their speed and torque (Shekher *et al.*, 2024; Alitasb, 2024), in order to improve their performance, by increasing the voltage in proportion to the required frequency, which necessitated the use of several control techniques. Conventional proportional integer (PI) control is widely used to control induction motors due to its precise and rapid control of their speed during variable operating conditions, especially in steady-state performance (Alitasb, 2024; Gaythri & Thivay Prasad, 2019; Kada *et al.*, 2021).

Recently, artificial neural network (ANN) has witnessed very wide use as a mathematical model inspired by biological neural networks, based on the working principle of human nerves, so that it included various fields; especially the field of induction motors (Mahfoud *et al.*, 2024; Junior *et al.*, 2022; Karami-Shahnani *et al.*, 2023). Neural networks are considered a promising approach that allows optimizing and developing control algorithms for asynchronous machines by learning from data, which allows the relationship between the inputs and outputs of the control system to be represented accurately and effectively (Mahfoud *et al.*, 2024; Barik & Jaladi, 2016; Kada *et al.*, 2020), and this is what makes them replace classical controllers.

In this work, three control strategies for induction motor, including current, electromagnetic torque and speed, have been proposed based on replacing the classical PI control (PI controller and decoupling by compensating the voltages of the vector control) by developed inverse ANNs. In order to determine the most efficient and high-performance IANN controller, a qualitative comparison was made between the results of these proposed strategies and those obtained from the

classical controller. MATLAB/SIMULINK software was used to develop the three-phase induction motor and various controller models as well as to verify the performance of these controllers.

2. Mathematical modeling

2.1. Dynamic model of IM and its vector control

In order to obtain a simpler formulation and reduce the complexity of the machine model, the establishment of its mathematical model was developed on the basis of simplifying hypotheses, namely that the machine is symmetrical, operates in unsaturated mode and that the various losses as well as the effect of the shock absorbers are negligible (Karami-Shahnani *et al.*, 2023).

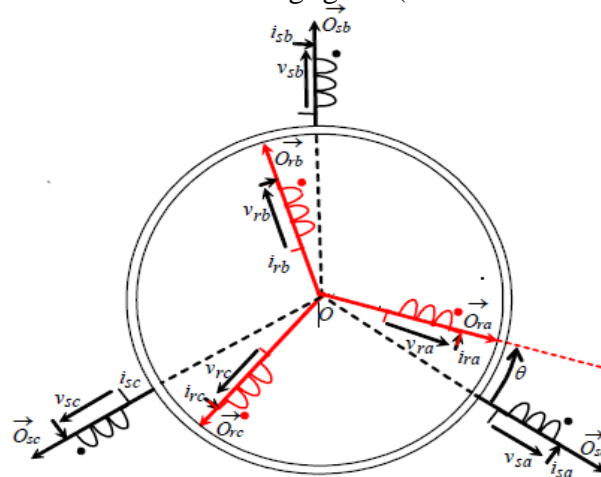


Figure 1 – Electrical representation of a three-phase asynchronous motor.

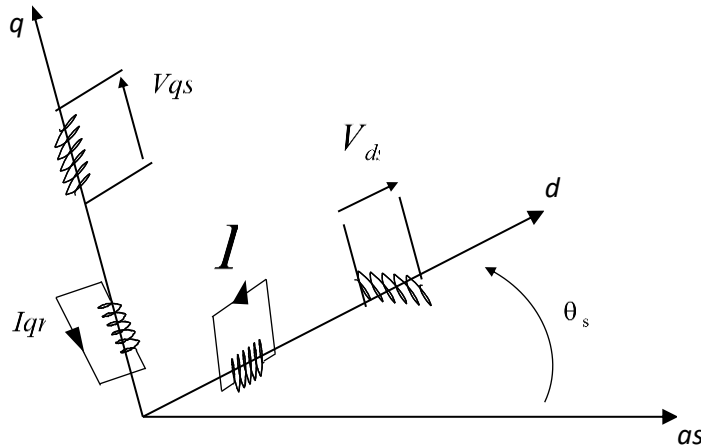


Figure 2 – d-q axes superimposed onto a three-phase IM.

The differential equations of the asynchronous motor in the abc frame are:

Stator and rotor voltage equation:

$$[V_{Sabc}] = \begin{bmatrix} v_{sa} \\ v_{sb} \\ v_{sc} \end{bmatrix}, \quad [I_{Sabc}] = \begin{bmatrix} i_{sa} \\ i_{sb} \\ i_{sc} \end{bmatrix}, \quad [\varphi_{Sabc}] = \begin{bmatrix} \varphi_{sa} \\ \varphi_{sb} \\ \varphi_{sc} \end{bmatrix} \quad (1)$$

$$[V_{rabc}] = \begin{bmatrix} v_{ra} = 0 \\ v_{rb} = 0 \\ v_{rc} = 0 \end{bmatrix}, \quad [I_{rabc}] = \begin{bmatrix} i_{ra} \\ i_{rb} \\ i_{rc} \end{bmatrix}, \quad [\varphi_{rabc}] = \begin{bmatrix} \varphi_{ra} \\ \varphi_{rb} \\ \varphi_{rc} \end{bmatrix} \quad (2)$$

Stator and rotor flux equation:

$$[\varphi_s] = [L_{ss}][I_s] + [M_{sr}]^T [I_r] \quad (3)$$

$$[\varphi_r] = [L_{rr}][I_r] + [M_{rs}]^T [I_s] \quad (4)$$

The relationship between the equations in the abc frame and the Park frame can be written as:

$$\begin{bmatrix} I_{ds} \\ I_{qs} \\ I_{os} \end{bmatrix} = [P(\theta_s)] \begin{bmatrix} I_{as} \\ I_{bs} \\ I_{cs} \end{bmatrix}, \begin{bmatrix} V_{ds} \\ V_{qs} \\ V_{os} \end{bmatrix} = [P(\theta_s)] \begin{bmatrix} V_{as} \\ V_{bs} \\ V_{cs} \end{bmatrix} \text{ et } \begin{bmatrix} \varphi_{ds} \\ \varphi_{qs} \\ \varphi_{os} \end{bmatrix} = [P(\theta_s)] \begin{bmatrix} \varphi_{as} \\ \varphi_{bs} \\ \varphi_{cs} \end{bmatrix}$$

Where $P(\theta)$ is the transformation matrix in the Park transform and given as follows:

$$[P(\theta)] = \frac{3}{2} \cdot \begin{bmatrix} \cos \theta & \cos\left(\theta - \frac{2\pi}{3}\right) & \cos\left(\theta - \frac{4\pi}{3}\right) \\ -\sin \theta & -\sin\left(\theta - \frac{2\pi}{3}\right) & -\sin\left(\theta - \frac{4\pi}{3}\right) \\ \frac{1}{\sqrt{2}} & \frac{1}{\sqrt{2}} & \frac{1}{\sqrt{2}} \end{bmatrix} \quad (5)$$

$$\begin{cases} V_{ds} = R_s I_{ds} + \frac{d\varphi_{ds}}{dt} - \frac{d\theta_s}{dt} \varphi_{qs} \\ V_{qs} = R_s I_{qs} + \frac{d\varphi_{qs}}{dt} + \frac{d\theta_s}{dt} \varphi_{ds} \\ 0 = R_r I_{dr} + \frac{d\varphi_{dr}}{dt} - \frac{d\theta_r}{dt} \varphi_{qr} \\ 0 = R_r I_{qr} + \frac{d\varphi_{qr}}{dt} + \frac{d\theta_r}{dt} \varphi_{dr} \end{cases} \quad (6)$$

$$\begin{cases} \varphi_{ds} = L_s I_{ds} + M I_{dr} \\ \varphi_{qs} = L_s I_{qs} + M I_{qr} \\ \varphi_{dr} = L_r I_{dr} + M I_{ds} \\ \varphi_{qr} = L_r I_{qr} + M I_{qs} \end{cases} \quad (7)$$

Where, $L_s = l_s - m_s$, $L_r = l_r - m_r$ et $M = L_m = \frac{3}{2} M_{sr}$ are the cyclic inductances stator, rotor and mutual, respectively.

The stator and rotor currents are given as a function of flux.

$$\begin{cases} I_{ds} = \frac{1}{\sigma L_s} \varphi_{ds} - \frac{M}{\sigma L_s L_r} \varphi_{dr} \\ I_{qs} = \frac{1}{\sigma L_s} \varphi_{qs} - \frac{M}{\sigma L_s L_r} \varphi_{qr} \\ I_{dr} = -\frac{M}{\sigma L_s L_r} \varphi_{ds} + \frac{1}{\sigma L_r} \varphi_{dr} \\ I_{qr} = -\frac{M}{\sigma L_s L_r} \varphi_{qs} + \frac{1}{\sigma L_r} \varphi_{qr} \end{cases} \quad (8)$$

Where $\sigma = 1 - \frac{M^2}{L_s L_r}$ is the dispersion coefficient.

The expression of the electromagnetic torque is given by:

$$C_e = \frac{3}{2} P \frac{M}{L_r} (\varphi_{dr} I_{qs} - \varphi_{qr} I_{ds}) \quad (9)$$

The objective of vector control is to find the decoupling between the flux and the electromagnetic torque. The principle of this control is based on the exploitation of the dynamic model of the motor and consists of choosing an axis system (d,q) and orienting it according to the rotor flux, by canceling the quadrature component φ_{qr} , to keep only the direct component φ_{dr} .

The rotor flux is then aligned on the direct axis and the magnetic equations become:

$$\varphi_{dr} = \varphi_r, \varphi_{qr} = 0 \quad (10)$$

This makes it possible to control the torque via the current I_{sq} and the flux using the current I_{sd} . The new expression for the electromagnetic torque can then be written:

$$C_e = P \frac{3L_m}{2L_r} (\varphi_r \cdot I_{qs}) \quad (11)$$

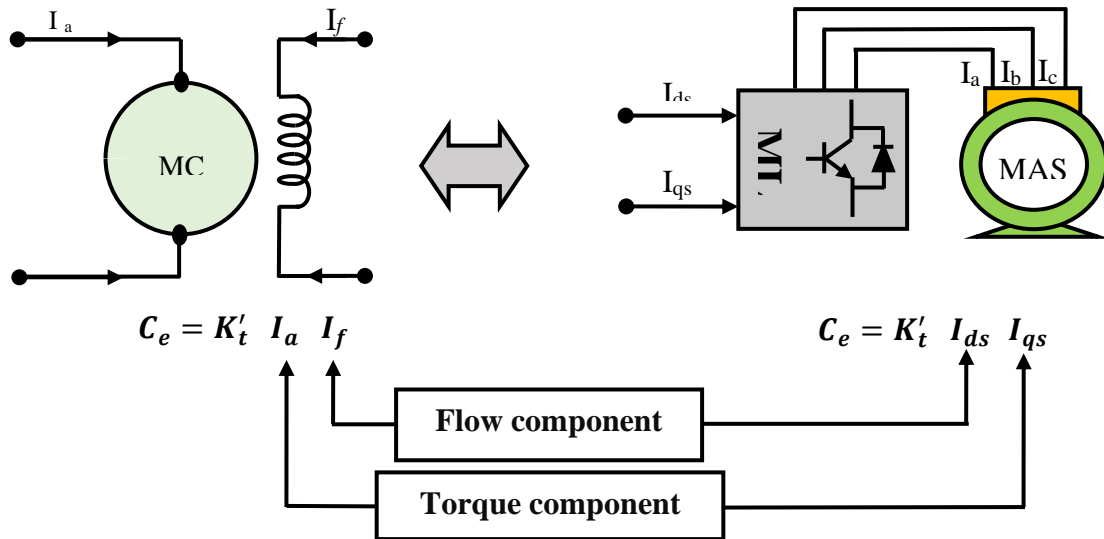


Figure 3 – Diagram of the decoupling principle for MAS by analogy with MCC.

2.2. Inverse artificial neural network model

The inverse artificial neural network (IANN) model plays an important role in systems control theory. The structure of the inverse ANN is shown in figure 4. As shown in this structure, and in order to reach the set-point, the ANN inverse is provided with the present and past inputs ($u(k-1)$, $u(k)$) and the desired set-point $y(k+1)$ as well as the past outputs ($y(k)$, $y(k-n+1)$), to predict the desired input $u(k)$ (Rajesh *et al.*, 2015).

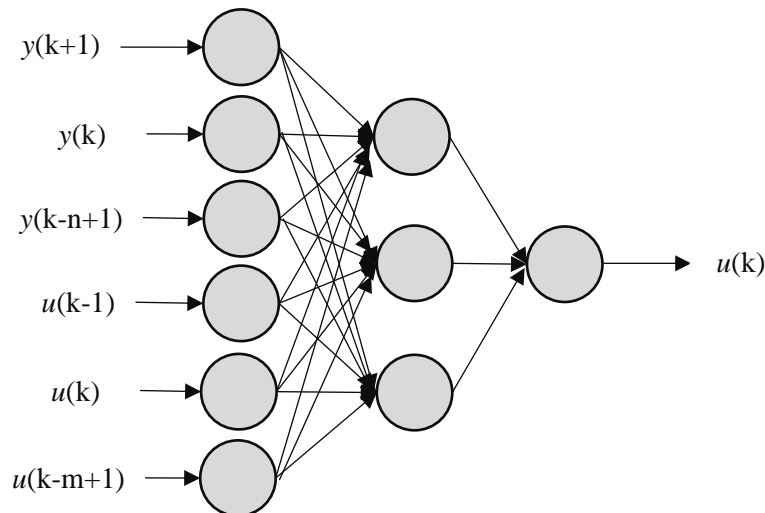


Figure 4 – Inverse ANN structure.

The dynamic system that links the inputs to the outputs of the inverse ANN can be described by equation 12:

$$y(k + 1) = f(y(k), \dots, y(k - n + 1), u(k), \dots, u(k - m + 1)) \quad (12)$$

Where the system's output $y(k+1)$ depends on the (n) previous values of the output and the (m) past values of the input. In general, the IANN model of this system can be presented in the following form:

$$u(k) = f^{-1}(y(k + 1), y(k), \dots, y(k - n + 1), u(k - 1), \dots, u(k - m)) \quad (13)$$

Where $u(k)$ and $y(k)$ are the inputs and outputs of this system, respectively, as well as the non-linear function f is supposed unknown. In this study, the focus was on the dynamic part of the system's response and the structure of the feed forward neural network model (FFNNM) shown in Figure 4 was adopted.

Multi-layer perceptron networks can be used to develop the inverse neural model of the system using MLP type. These MLP networks present the simplest solution, however the representation of the dynamic aspect of the system remains problematic. Applying delays to the input layer of this type of network can provide the solution to remedy the static aspect of MLPs. This solution has the advantage of allowing the application of the traditional gradient back-propagation algorithm for learning multi-layer networks (Kada *et al.*, 2020; Salem *et al.*, 2007). Figure 5 shows the general learning architecture of IANNs.

The parameters of the FFNN model are estimated using the back-propagation algorithm and the criterion to respect minimized is given by:

$$E(w) = \sum_{k=1}^n ((u(k) - \hat{u}(k, w))^2) \quad (14)$$

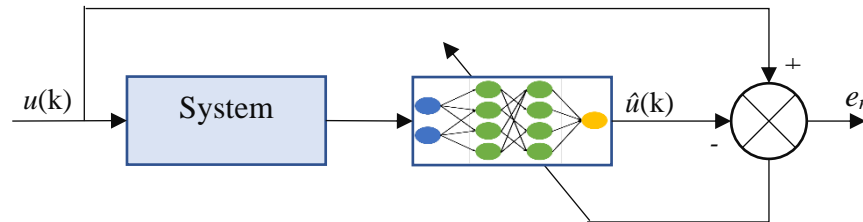


Figure 5 – General learning architecture.

3. Simulation details

To test the efficiency and performance of the proposed control strategies for a three-phase asynchronous motor, as an asynchronous machine (induction machine), which has the parameters shown in Table 1, numerical simulations were performed under MATLAB/Simulink software. Figure 6 represents the complete structural blocks of this asynchronous machine, PI controller and vector control which are based on their mathematical models. To carry out this study, IANNs were developed to replace the PI controller and decoupling by compensating the voltages (V_{ds} et V_{qs}) of the vector control. These IANNs were learned from simulation results obtained by classical control system (PI controller and vector control) with back propagation learning algorithm. The three control strategies proposed in this study are based on replacing PI controller, vector control and PI with vector control by the developed inverse ANNs, respectively. In order to properly test these control strategies, a resistive torque of 10 N.m was applied and eliminated on our system in moments 1s and 2s respectively for a speed setpoint of 100 rad/sec.

control system (PI controller and vector control), while the torque depends only on the quadrature component I_{qs} . This shows that the stator current has been decomposed into two terms corresponding to flux and torque respectively, and as a result a structure similar to that of a direct current (DC) machine is obtained.

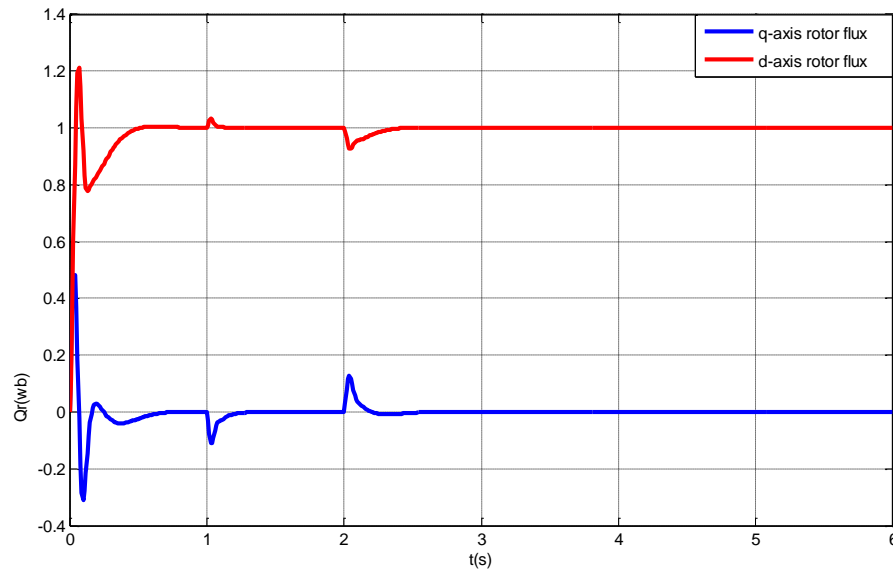


Figure 8 – Rotor flux vectors vs time.

The different responses (Figures 11, 12 and 13 in red) of the classical control system show rapid rejection of load disturbances with zero overshoot rate and negligible error at steady state. The results obtained by simulating the behavior of the classical control system of this induction machine were exploited to develop the two inverse ANNs.

Figure 9 shows the developed architectures for the inverse ANN controller and the inverse ANN control respectively, as well as performance details and analysis parameters. Figures 10-a and 10-b present the evolution of the quadratic errors as a function of iteration number for the developed IANNs. According to these results, the quadratic errors have a non-linear evolution characterized by a slope at the beginning, i.e. a high convergence speed, then it becomes slower and slower, and the latter decreasing depending on the number of iterations.

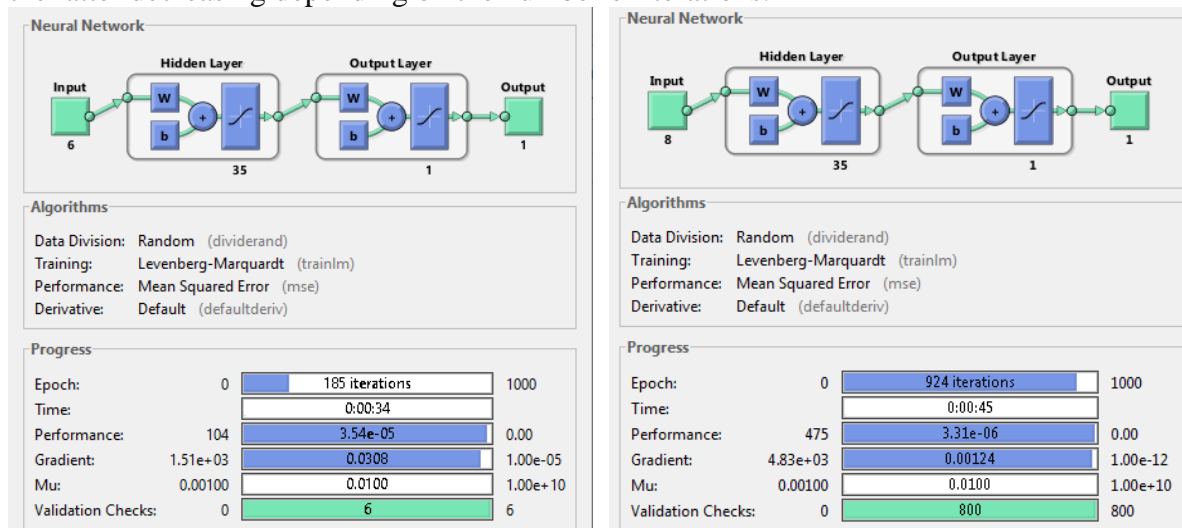


Figure 9 – IANNs architecture for, a) PI Controller (ANN Controller), b) vector control (ANN Control).

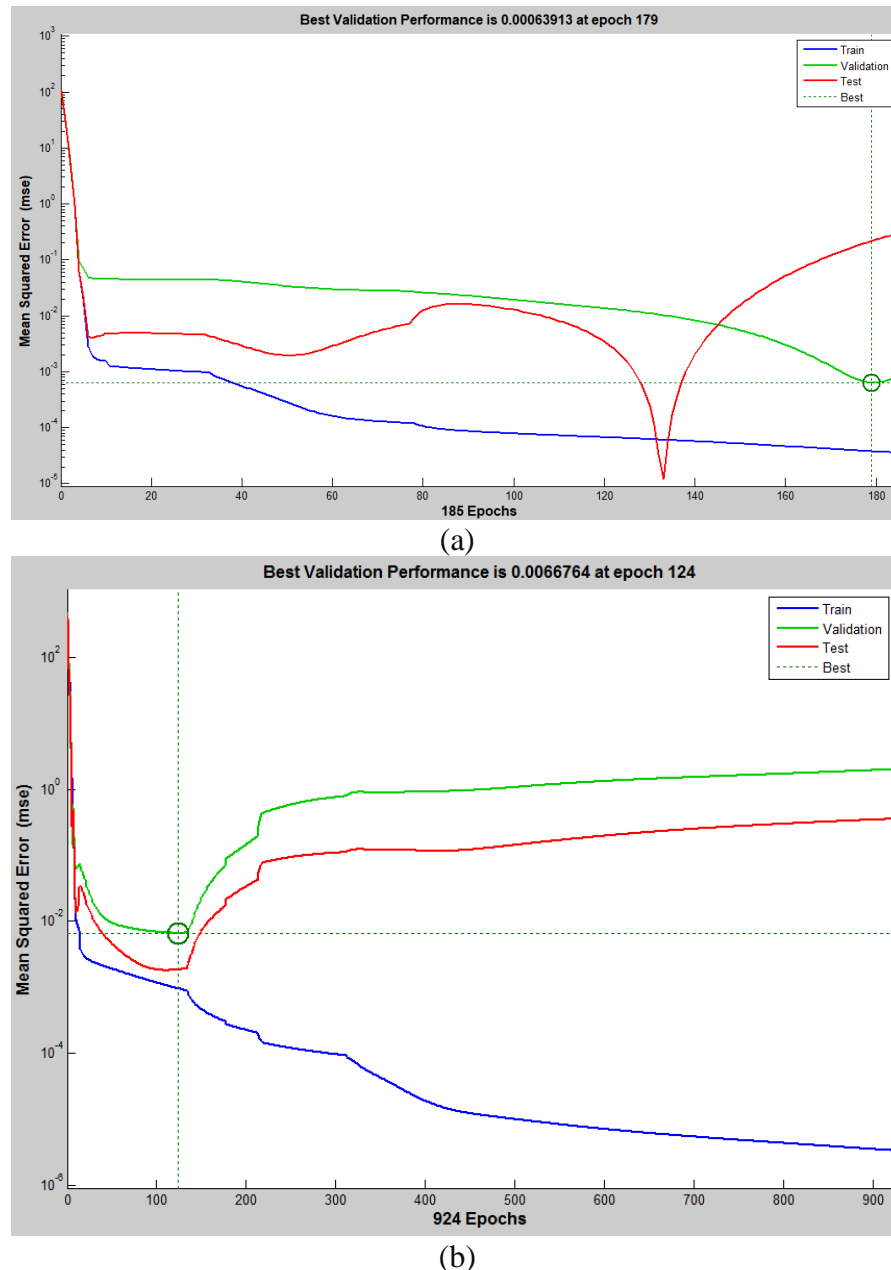


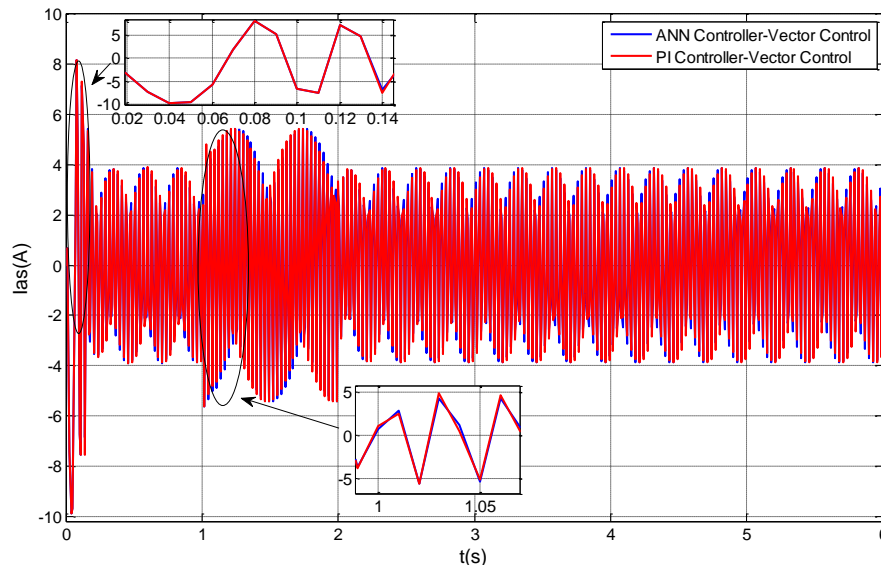
Figure 10 – IANNs performance diagram for current, torque and speed data, a) ANN Controller, b) ANN Control.

According to the results obtained, in conventional control and various control strategies based on inverse ANNs, the current with which the motor starts is double the current that supplies the motor in the steady state and this does not represent any risk to the motor because its duration is short. The electromagnetic torque also pulsates strongly at the first moment of starting the machine, and this phenomenon is reflected by the presence of noise generated by the mechanical part (moment of inertia), it reaches the no-load regime. The rotation speed of this machine is decreased when a resistive torque is applied and increases when this torque is released, then this speed returns to the reference value 100rad/s.

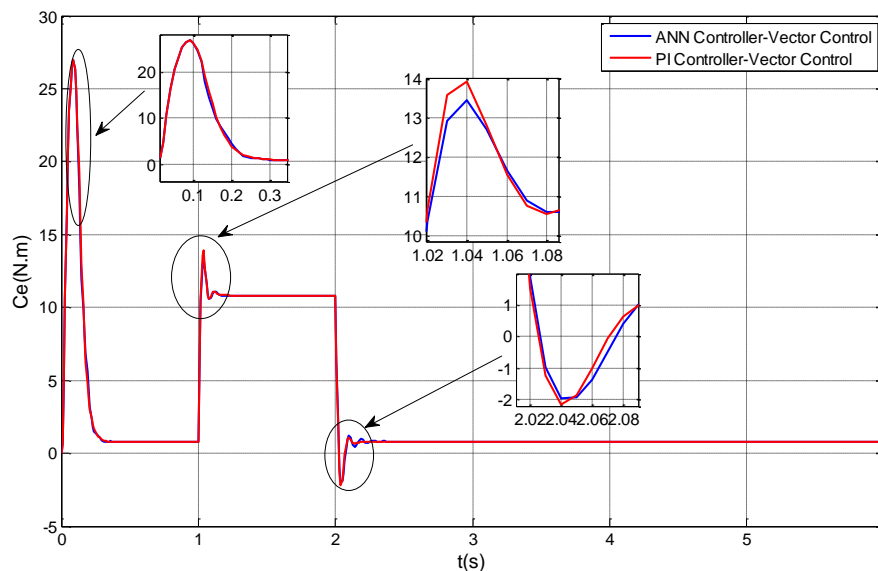
In the case of replacing the PI controller (of the classic control) by its inverse neural network (ANN controller) and the starting moment of the induction machine: The stator inrush currents increase to 8.178 A and 8.15 A for the classical control and the neural controller respectively, as shown in Figure 11-a, due to the increase in load torque. The electromagnetic torque of the conventional control is strongly pulsating with a peak value of 26.96N.m and for the neural controller the peak value of the torque is 26.9N.m. With the application and elimination of resistive

torque, the current and electromagnetic torque values of the neural controller are slightly lower compared to the conventional control as shown in Table 2. These results show that the ANN controller reduces the risks on the machine in the different operating regimes.

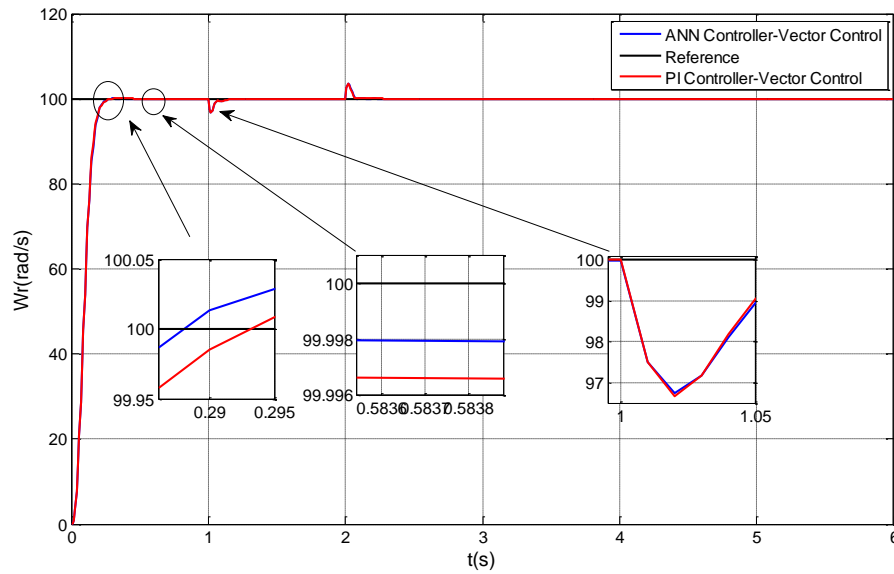
Figure 11-c shows the evolution of the speed of the asynchronous machine as a function of time. This figure shows that the neural controller is characterized by a slightly better response time compared to the conventional control (Table 2). The application of torque results in a decrease in motor speed of 96.7 rad/s - 96.74 rad/s for the conventional control system and the nervous control system respectively. On the other hand, with the removal of this torque, the speed increases to 103.459 rad/s – 103.54 rad/s.



(a)



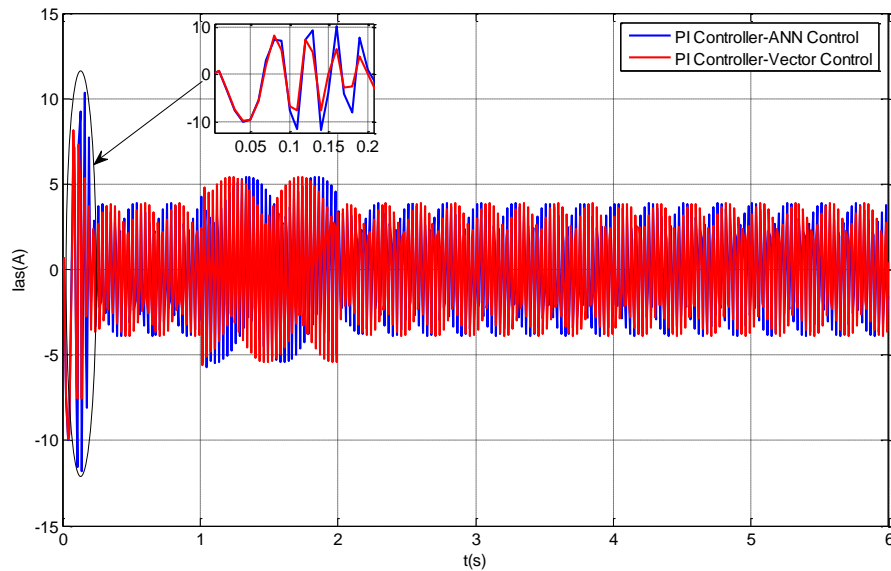
(b)



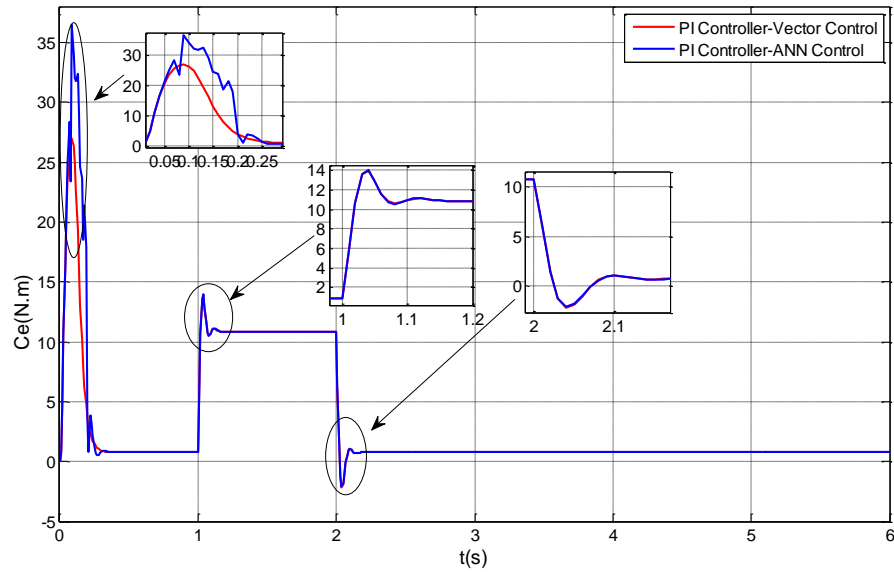
(c)

Figure 11 – Classical Control and ANN-Controller/Vector-Control responses, a) Current I_{as} , b) Electromagnetic torque C_e , c) Speed W_r .

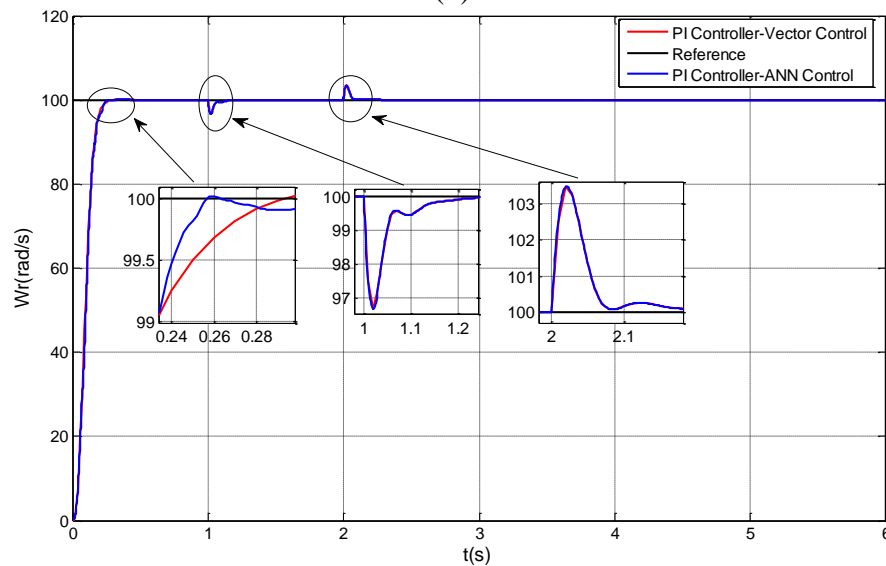
In the case of the strategy based on the replacement of the vector control by the ANN control, and at the instant of starting the machine, the current and the electromagnetic torque of this strategy have higher values compared to the classical control. When applying resistive torque, these values of the ANN control are very close to those of the classical control, which shows that this strategy provides less protection for the induction motor from risks than the classical control, especially during the start-up of this machine. From Figure 12-c and table 2, the inverse artificial neural network control has a relatively fast response compared to the classical control.



(a)



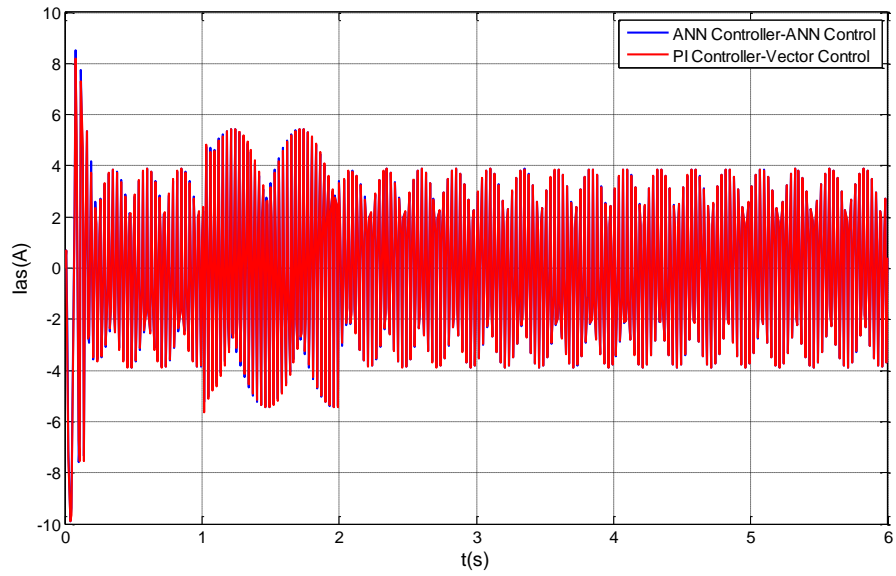
(b)



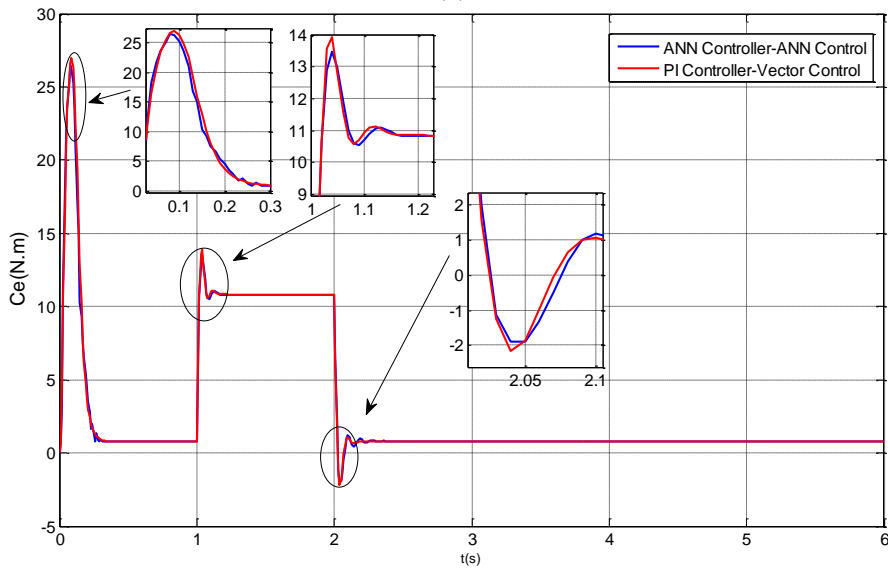
(c)

Figure 12 – Classical Control and PI-Controller/ANN-Control responses, a) Current I_{as} , b) Electromagnetic torque C_e , c) Speed W_r .

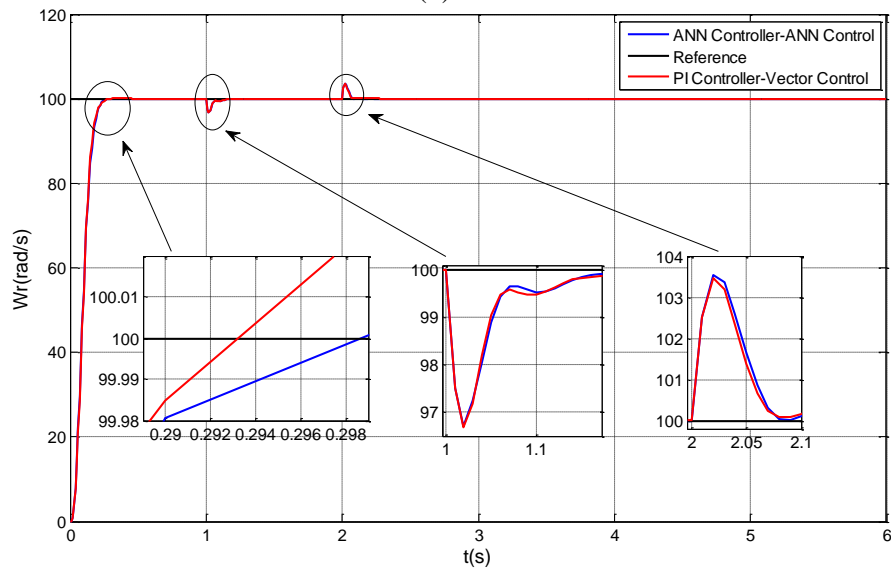
In the control technique which uses two inverse neural networks replacing the PI controller and the decoupling by compensating the voltages of the vector control, the current of this technique is significantly important compared to the conventional control when starting the machine, which shows that the classical control is distinguished by its efficiency and better protects the machine from risks. On the other hand, during the rest of the operating times, the values of this current and electromagnetic torque for the ANN controller/ANN control and the conventional control are very similar, as well as the response time of both control systems (Table 2).



(a)



(b)



(c)

Figure 13 – Classical Control and ANN-Controller/ANN-Control responses, a) Current I_{as} , b) Electromagnetic torque C_e , c) Speed W_r .

According to the different results obtained, the control strategies developed in this study, which are based on inverse artificial neural networks, have proven their effectiveness and worthiness to replace classical control, especially during the steady state operation of this induction motor. In addition, the ANN controller/vector control strategy is considered a good proposed control technique for the asynchronous machine in terms of low consumption current and electromagnetic torque, as well as its good fast response compared to other proposed strategies.

Table 2 – Basic parameters of the control systems.

Parameters	Time	PI Controller- Vector Control	ANN Controller- Vector Control	PI Controller – ANN Control	ANN Controller – ANN Control
Current (A)	t=0s	8.178	8.15	10.3	11.1
	t=1s *	4.809	4.18	4.23	4.06
	t=2s #	3.332	2.82	3.38	3.2
Torque (N.m)	t=0s	26.96	26.9	36.3	26.51
	t=1s *	13.918	13.44	13.95	13.47
	t=2s #	-2.168	-1.955	-2.094	-1.895
Speed (rad/s)	t=0s	98.6	98.7	98.5	98.9
	t=1s *	96.7	96.74	96.68	96.7
	t=2s #	103.459	103.54	103.45	103.35
Response time (s)		0.2932	0.288	0.2567	0.292

* Application of the resistant torque (10N.m). # Elimination of the resisting torque

5. Conclusion

In this paper, inverse artificial neural networks (IANNs) are developed in order to replace the PI controller and vector control of classical controller with the aim of improving the tracking performance of induction motor. These networks were trained from induction motor responses, current, torque and speed, using the classical controller in order to reach at their optimal architectures with very small prediction error. The control technique using inverse neural networks allows the speed to be little affected by disturbances and to track its set point, which lends itself well to adjusting the speed of this asynchronous motor, as well as ensuring good orientation of the rotor flux. These IANNs architectures have made it possible, on the one hand, to improve the dynamic and static performances of the machine and, on the other hand, to ensure robustness against disturbances, giving it a wide application in the field of electric drive.

REFERENCES

- Alitasb, G., K. (2024). Integer PI, fractional PI and fractional PI data trained ANFIS speed controllers for indirect field oriented control of induction motor. *Heliyon*. 10, e37822. DOI: [10.1016/j.heliyon.2024.e37822](https://doi.org/10.1016/j.heliyon.2024.e37822)
- Atif, M., Azmat, S., Khan, F., Albogamy, F., R., Khan, A. (2024). AI-Driven Thermography-based Fault Diagnosis in Single-Phase Induction Motor. *Results in Engineering*, 24, 103493. DOI: [10.1016/j.rineng.2024.103493](https://doi.org/10.1016/j.rineng.2024.103493)
- Barik, S., K., Jaladi, K., K. (2016). Five-phase induction motor DTC-SVM scheme with PI controller and ANN controller. *Procedia Technol*, 25, 816–823. DOI: [10.1016/j.protcy.2016.08.184](https://doi.org/10.1016/j.protcy.2016.08.184)
- Chandrasekaran, G., Karthikeyan, P., R., Kumar, N., S., Kumarasamy, V. (2021). Test scheduling of System-on-Chip using Dragonfly and Ant Lion optimization algorithms. *J Intell Fuzzy Syst*, 40, 4905–4917. DOI: [10.3233/JIFS-201691](https://doi.org/10.3233/JIFS-201691)

- EL-Merrassi, W., Abounada, A., Ramzi, M. (2022). Performance analysis of novel robust ANN-MRAS observer applied to induction motor drive. *Int J Syst Assur Eng Manag*, 13(4), 2011–2028. DOI: [10.1007/s13198-021-01614-w](https://doi.org/10.1007/s13198-021-01614-w)
- Gaythri, B., Thivay Prasad, D. (2019). Control Induction Motor using Neural Network. *International Resurach Journal of Engineering and Technology*, 6(8), 837-844.
- Junior, R., F., R., dos Santos Areias, I., A., Campos, M., M., Teixeira, C., E., C.E. da Silva, C., E., Gomes G., F. (2022). Fault detection and diagnosis in electric motors using 1D convolutional neural networks with multi-channel vibration signals. *Measurement*, 190, 110759. DOI: [10.1016/j.measurement.2022.110759](https://doi.org/10.1016/j.measurement.2022.110759)
- Kada, B., El-Kebir, A., Negadi, K., Belhadj, H., Chaouch, D., E. (2020). Application of Adaptive Controller Neural Network Based on RBF NN for Temperature Control Electrical Resistance Furnace. *Przeglad Elektrotechniczny*. 96(6), 33. DOI: [10.15199/48.2020.06.06](https://doi.org/10.15199/48.2020.06.06)
- Kada, B., El Kebir, A., Berka, M., Belhadj, H., Chaouch, D., E. (2021). Study of designing regulator for temperature electrical resistance furnace using Kalman stochastic reconstructor. *Indonesian Journal of Electrical Engineering and Computer Science*, 24(1), 134-143. DOI: [10.11591/ijeecs.v24.i1.pp134-143](https://doi.org/10.11591/ijeecs.v24.i1.pp134-143)
- Karami-Shahnani, A, Dehghan-Niri, H., Nasiri-Zarandi, R., Abbaszadeh, K., Toulabi, M., S. (2023). Online inductance estimation of pm-assisted synchronous reluctance motor using artificial neural network. In 2023 14th Power Electronics, Drive Systems, and Technologies Conference (PEDSTC) (pp. 1–6). IEEE. DOI: [10.1109/PEDSTC57673.2023.10087136](https://doi.org/10.1109/PEDSTC57673.2023.10087136)
- Kouadria, M., Chedjara, Z., Benbouzid, M., Su, C., L., Guerrero, J., M., Babul Salam KSM Kader Ibrahim, Ahmed, H. (2024). A zoomed root-Prony technique for efficient bearing fault detection in induction motors. *Results in Engineering*, 24, 103367. DOI: [/10.1016/j.rineng.2024.103367](https://doi.org/10.1016/j.rineng.2024.103367)
- Mahfoud, S., El Ouanjli, N., Derouich, A., El Idrissi, A., Hilali, A., Chetouani, E. (2024). Higher performance enhancement of direct torque control by using artificial neural networks for doubly fed induction motor. *e-Prime - Advances in Electrical Engineering, Electronics and Energy*, 8, 100537. DOI: [10.1016/j.prime.2024.100537](https://doi.org/10.1016/j.prime.2024.100537)
- Mekrini, Z., Bri, S. (2018). High - Performance using Neural Networks in Direct Torque Control for Asynchronous Machine. *International Journal of Electrical and Computer Engineering (IJECE)*, 8(2), 1010-1017. DOI: [10.11591/ijece.v8i2.pp1010-101](https://doi.org/10.11591/ijece.v8i2.pp1010-101)
- Rajesh, R., J., Preethi, R., Mehata, P., Pandian, J. (2015). Artificial Neural Network Based Inverse ModelControl Of A Nonlinear Process. In 2015 International Conference on Computer, Communication and Control (IC4-2015). IEEE. DOI: [10.1109/IC4.2015.7375581](https://doi.org/10.1109/IC4.2015.7375581)
- Salem, M., Chaouch, D., E., Fayçal Khelfi, M. (2007). Inverse neural control of nonlinear systems. In 2007 4th International Conference on Computer Integrated Manufacturing (CIP'2007).
- Shekher, V., Sisodiya, A., Sinha, A., K., Harsh, H., Soren, N. (2024). Optimal tuning of PID controller for V/f control of Linear Induction Motor using Artificial Biological Intelligence. *Franklin Open*, 9, 100183. DOI: [0.1016/j.fraope.2024.100183](https://doi.org/0.1016/j.fraope.2024.100183)